

Gas stripping in galaxy groups – the case of the starburst spiral NGC 2276

Jesper Rasmussen,^{1*} Trevor J. Ponman¹ and John S. Mulchaey²

¹*School of Physics and Astronomy, University of Birmingham, Edgbaston, Birmingham B15 2TT*

²*Observatories of the Carnegie Institution, 813 Santa Barbara Street, Pasadena, California, USA*

Accepted —. Received —; in original form —

ABSTRACT

Ram pressure stripping of galactic gas is generally assumed to be inefficient in galaxy groups due to the relatively low density of the intragroup medium and the small velocity dispersions of groups. To test this assumption, we obtained *Chandra* X-ray data of the starbursting spiral NGC 2276 in the NGC 2300 group of galaxies, a candidate for a strong galaxy interaction with hot intragroup gas. The data reveal a shock-like feature along the western edge of the galaxy and a low-surface-brightness tail extending to the east, similar to the morphology seen in other wavebands. Spatially resolved spectroscopy shows that the data are consistent with intragroup gas being pressurized at the leading western edge of NGC 2276 due to the galaxy moving supersonically through the intragroup medium at a velocity ~ 850 km s⁻¹. Detailed modelling of the gravitational potential of NGC 2276 shows that the resulting ram-pressure could significantly affect the morphology of the outer gas disc but is probably insufficient to strip large amounts of cold gas from the disc. We estimate the mass loss rates due to turbulent viscous stripping and starburst outflows being swept back by ram pressure, showing that both mechanisms could plausibly explain the presence of the X-ray tail. Comparison to existing HI measurements shows that most of the gas escaping the galaxy is in a hot phase. With a total mass loss rate of $\sim 5 M_{\odot}$ yr⁻¹, the galaxy could be losing its entire present HI supply within a Gyr. This demonstrates that the removal of galactic gas through interactions with a hot intragroup medium can occur rapidly enough to transform the morphology of galaxies in groups. Implications of this for galaxy evolution in groups and clusters are briefly discussed.

Key words: galaxies: evolution — galaxies: individual: NGC 2276 — galaxies: interactions — galaxies: spiral — X-rays: galaxies — X-rays: galaxies: clusters

1 INTRODUCTION

There is a long standing argument about which processes are the key ones in modifying the morphology of galaxies in dense environments, and establishing the morphology-density relation and the associated truncation of star formation (see, e.g., Goto et al. 2003). Candidate processes for the morphological evolution of disc galaxies into lenticulars include ram pressure stripping, tidal stripping, galaxy harassment, strangulation, interaction-induced star formation, and major and minor mergers. Of these, the first two mechanisms have been extensively studied using both observational (e.g. Vogt et al. 2004) and numerical approaches (Abadi, Moore & Bower 1999; Stevens, Acreman & Ponman 1999; Quilis, Moore & Bower 2000; Roediger & Hensler 2005). In particular, recent HI

and X-ray observations of individual cluster galaxies have uncovered strong evidence for ongoing ram-pressure stripping (e.g. Vollmer et al. 2004; Wang, Owen & Ledlow 2004; Sun & Vikhlinin 2005).

While most studies of gas stripping have focused on galaxies in clusters, including the statistical approach presented by Goto (2005), there is growing evidence that much of the modification of galaxy morphologies and truncation of star formation actually takes place in groups and cluster outskirts rather than in the dense cluster cores (Lewis et al. 2002; Helsdon & Ponman 2003; Gonzales et al. 2005; Homeier et al. 2006). This has been interpreted by many authors as ruling out the possibility that stripping via interactions with a hot intracluster medium (ICM) plays a major role in morphological transformations, given that it is expected to be much less effective in poor systems than in the cores of rich clusters. This interpretation remains to be tested by direct observations, however, and recently, claims

* E-mail: jesper@star.sr.bham.ac.uk

have been made for X-ray (Sivakoff, Sarazin & Carlin 2004; see also Machacek et al. 2005b) and HI (Bureau & Carignan 2002; Kantharia et al. 2005) evidence of ram-pressure stripping in groups. But, as noted by these authors, ram-pressure stripping is not the only viable explanation for the gas morphology seen in these systems. One problem with assessing the importance of ram pressure in these cases is that of obtaining robust constraints on the true 3-D velocity of the galaxy through the intragroup medium.

In an attempt to investigate the efficiency of gas removal in groups, and in particular test whether gas stripping through ICM interactions can in fact be effective in group environments, we obtained *Chandra* data of the spiral NGC 2276 in the NGC 2300 group of galaxies. This galaxy displays a disturbed optical morphology and constitutes another good candidate for a strong interaction with hot intragroup gas. NGC 2300 itself is the central elliptical in a sparse group catalogued with just four galaxies (Giudice 1999), this group being the first in which an X-ray emitting intragroup medium (IGM) was detected (Mulchaey et al. 1993). The peculiar morphology of NGC 2276 has also attracted attention, spawning detailed studies of its optical, radio, and X-ray point source properties (Gruendl et al. 1993; Hummel & Beck 1995; Davis et al. 1997; Davis & Mushotzky 2004). The distributions of optical light, HI gas, and radio continuum emission in this galaxy show a bow-shock-like structure along the western edge, which may suggest a shocked gas component. If so, the galaxy must be moving supersonically through the ambient IGM. Evidence supporting this interpretation is the high star formation rate of NGC 2276 ($\sim 5 M_{\odot} \text{ yr}^{-1}$; Davis et al. 1997), with much of this starburst activity occurring along the western edge, as expected if an interaction with the IGM has triggered some of the star formation via ram pressure compression of molecular gas.

Also, similarly to many of the Virgo cluster spirals showing signs of ICM interactions (Cayatte et al. 1990), there is evidence that NGC 2276 is deficient in HI compared to spirals in the field. For an isolated spiral of the same morphology and optical luminosity, the relation of Haynes & Giovanelli (1984) would predict an HI content $M_{\text{HI,pred.}} \approx 1.4 \times 10^{10} M_{\odot}$, which is 2.2 times the observed amount of $M_{\text{HI,obs.}} \approx 6.4 \times 10^9 M_{\odot}$ (Young et al. 1989; corrected to the adopted distance of 36.8 Mpc, see below). This corresponds to an HI deficiency, as defined by Verdes-Montenegro et al. (2001), of $\log M_{\text{HI,pred.}} - \log M_{\text{HI,obs.}} \approx 0.35$, and suggests that NGC 2276 may already have lost a significant fraction of its original (i.e. prior to infall into the group) gas content.

To estimate the pressure conditions across the possible shock front and settle the question of whether a bow shock is really present in NGC 2276, X-ray data of high spatial resolution remain the only viable means. These can enable constraints to be placed on the 3-D velocity of the galaxy and allow a test of whether the conditions for ram-pressure stripping are met. This is the goal of the present study. To this end, we use *Chandra* data to map out the detailed spectral and spatial features of hot gas in and around NGC 2276 and NGC 2300. Salient features of the observed group galaxies are listed in Table 1.

Adopting $H_0 = 75 \text{ km s}^{-1} \text{ Mpc}^{-1}$, the distance to NGC 2276 is 36.8 Mpc (Tully 1988), with 1 arcmin cor-

Table 1. Properties of observed galaxies. *B*- and *K*-band luminosities L_B and L_K calculated from (extinction-corrected) apparent magnitudes listed in Tully (1988) and the NASA/IPAC Extragalactic Database (NED), respectively. Stellar masses M_* computed using the prescription of Mannucci et al. (2005). Morphologies and recession velocities v_r (corrected for Virgocentric infall) from the HyperLeda database.

Galaxy	NGC 2276	NGC 2300
RA (J2000)	07 27 11.42	07 32 20.05
Dec (J2000)	+85 45 19.0	+85 42 31.4
Hubble type	SBc	E3
$L_B (L_{B,\odot})$	4.4×10^{10}	4.2×10^{10}
$L_K (L_{K,\odot})$	7.0×10^{10}	2.7×10^{11}
$M_* (M_{\odot})$	2.7×10^{10}	2.1×10^{11}
$v_r (\text{km s}^{-1})$	2684	2263

responding to 10.7 kpc. All errors are quoted at 90 per cent confidence unless stated otherwise.

2 OBSERVATIONS AND ANALYSIS

2.1 Data preparation

NGC 2276 was observed by *Chandra* (obs. ID 4968) with the ACIS-S3 chip as aimpoint, for an effective exposure time of 45.8 ks, and with the CCDs at a temperature of -120° C . The nearby group elliptical NGC 2300, which is the brightest group galaxy, was located on the S2 chip. The two other galaxies in the group, NGC 2268 and IC 455, are not covered by this *Chandra* pointing. A fifth galaxy, UGC 03670, with a distance to NGC 2300 of 16 arcmin ($\sim 170 \text{ kpc}$), has a redshift concordant with the other group galaxies and is probably yet another group member. This galaxy is located on the I3 chip; showing only very faint X-ray emission it will not be discussed further here, where we will concentrate on the emission on the S2 and S3 chips.

Data were telemetered in Very Faint mode which allows for a superior suppression of background events, so calibrated event lists were regenerated and background screened using the ACIS_PROCESS_EVENTS tool in CIAO v3.2. Bad pixels were screened out using the bad pixel map provided by the pipeline, and remaining events were grade filtered, excluding *ASCA* grades 1, 5, and 7. Periods of high background were identified using 3σ clipping of full-chip lightcurves, binned in time bins of length 259.8-s and extracted in off-source regions in the 2.5–7 keV band for back-illuminated chips and in 0.3–12 keV for front-illuminated chips. These periods were excluded from the data, leaving a cleaned exposure time of 44.2 ks. Blank-sky background data from the calibration database were screened and filtered as for source data.

Point source searches were carried out with WAVDETECT using a range of scales and detection thresholds. Results were combined, yielding a total of 112 detected sources, 75 of which are located on the S2 and S3 chips used in this analysis. Source extents were quantified using the 4σ detection ellipses from WAVDETECT, and these regions were masked out in all subsequent analysis.

The *Chandra* astrometry was checked against the op-

tical position of NGC 2300 as listed in NED, revealing no significant difference.

2.2 Imaging and spectral analysis

Full-resolution ($0.5 \text{ arcsec pixel}^{-1}$) adaptively smoothed, background subtracted images are shown in Fig. 1. To produce these, background maps were generated from blank-sky data, and scaled to match the source count rates in source-free regions on the relevant chip. They were then smoothed to the same spatial scales as the source data and subtracted from the latter. The resulting images were finally exposure corrected using similarly smoothed, spectrally weighted exposure maps, with weights derived from spectral fits to the integrated diffuse emission. We stress that the resulting images served illustration purposes only and were not used for any quantitative analyses.

All spectra were accumulated in bins containing at least 25 net counts and fitted in XSPEC v11.3 assuming the solar abundance table of Grevesse & Sauval (1998). For the absorbing component we assumed the Galactic value of $N_{\text{H}} = 5.5 \times 10^{20} \text{ cm}^{-2}$ from Dickey & Lockman (1990). Spectral response files were generated using the MKACISRMF tool in CIAO v3.2, and all response products were weighted iteratively by a model of the incident source spectrum.

We employed two methods for generating background spectra. As IGM emission is expected to cover the S3 chip and thus must be subtracted from source spectra, background spectra for NGC 2276 were estimated from source-free regions on the same chip, described below. Since vignetting differences between the adopted source and background regions are small (~ 3 per cent at the peak spectral energy of $\sim 0.7 \text{ keV}$ for the region covered by the NGC 2276 disc), results are in any case likely to be dominated by statistical uncertainties. However, in cases where the properties of the IGM emission itself are of interest, we used blank-sky background data to generate background spectra. These data were scaled to match the 10–12 keV count rates of our source data in off-source regions on the S3 chip. Since the assumed value of N_{H} of our source data is a factor of ~ 4 larger than the exposure-weighted mean value of the relevant blank-sky files, the background is likely to be overestimated at low energies with this method. Consequently, when using blank-sky data for background estimation, we restricted spectral fitting to the 0.7–5 keV band, within which no systematic residuals were seen.

The regions used for spectral extraction are shown in Fig. 2, and a summary of fit results is provided in Table 2. A detailed investigation of the properties of hot gas in the elliptical NGC 2300 will be presented elsewhere.

3 RESULTS

3.1 NGC 2276

In the 0.3–5 keV band, roughly 1500 net counts are detected from diffuse emission in the NGC 2276 disc (inside region A in Fig. 2). The X-ray contours of the diffuse emission, as revealed by Fig. 1c, are clearly compressed at the western edge, demonstrating, as already indicated by earlier *ROSAT* HRI data (Davis et al. 1997), that also the *hot* gas in the disc

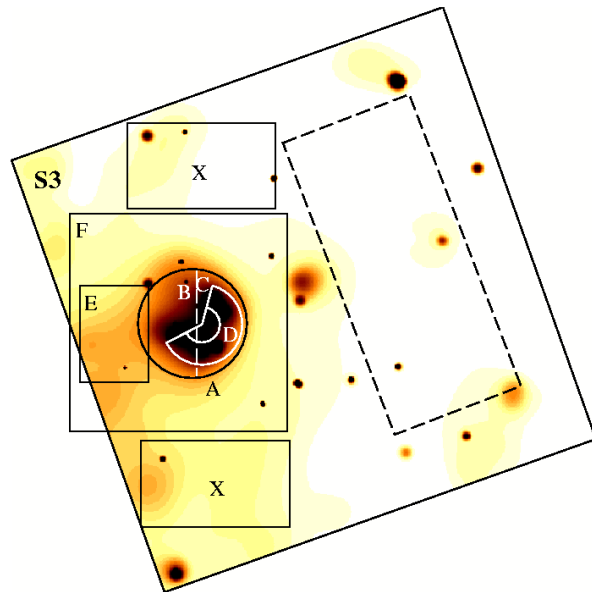


Figure 2. Regions used for spectral fitting of NGC 2276. For clarity, excluded point source regions are not shown. Dashed box outlines the region used for extraction of on-chip background spectra.

displays a disturbed morphology reminiscent of a bow-shock. A low-surface-brightness tail extending to the south-east is also visible. Smoothing the data to lower significances did not reveal evidence of any additional features in the diffuse emission.

The smoothed image also shows evidence for diffuse emission extending beyond the western optical edge of the galaxy. To investigate this in more detail, a surface brightness profile for the unsmoothed diffuse emission was extracted across the edge, inside the region shown as a dashed box in Fig. 1c. The result is plotted in Fig. 3, revealing a steep decline in X-ray surface brightness which coincides with the edge of the optical disc. Interestingly, there is indeed evidence for excess emission immediately outside this edge, extending to a few kpc from the optical disc. We will return to this feature in Section 4.1.

For the spectral analysis, the background was evaluated inside the dashed box shown in Fig. 2. Since this region is further from NGC 2300 and hence the IGM emission peak (Davis et al. 1996) than NGC 2276 itself, any gradient in the IGM surface brightness would imply that we could be underestimating the background at the position of NGC 2276. To test this, background spectra were also extracted from smaller regions in the immediate vicinity of NGC 2276 (regions X in Fig. 2), but the spectral results for the disc emission were found to be indistinguishable at the 1σ level for all fitted parameters.

A single-temperature fit to the disc emission (region A in Fig. 2) was found to be only marginally acceptable. Given the vigorous star formation in the disc, there could be a significant contribution from a population of unresolved high-mass X-ray binaries, or, as seen in many other starburst galaxies, evidence for a second thermal plasma component. We therefore also tried adding a power-law or a second thermal component, which both produced better fits ($\Delta\chi^2 = 13.5$ and 17.5, respectively, for 50 degrees of free-

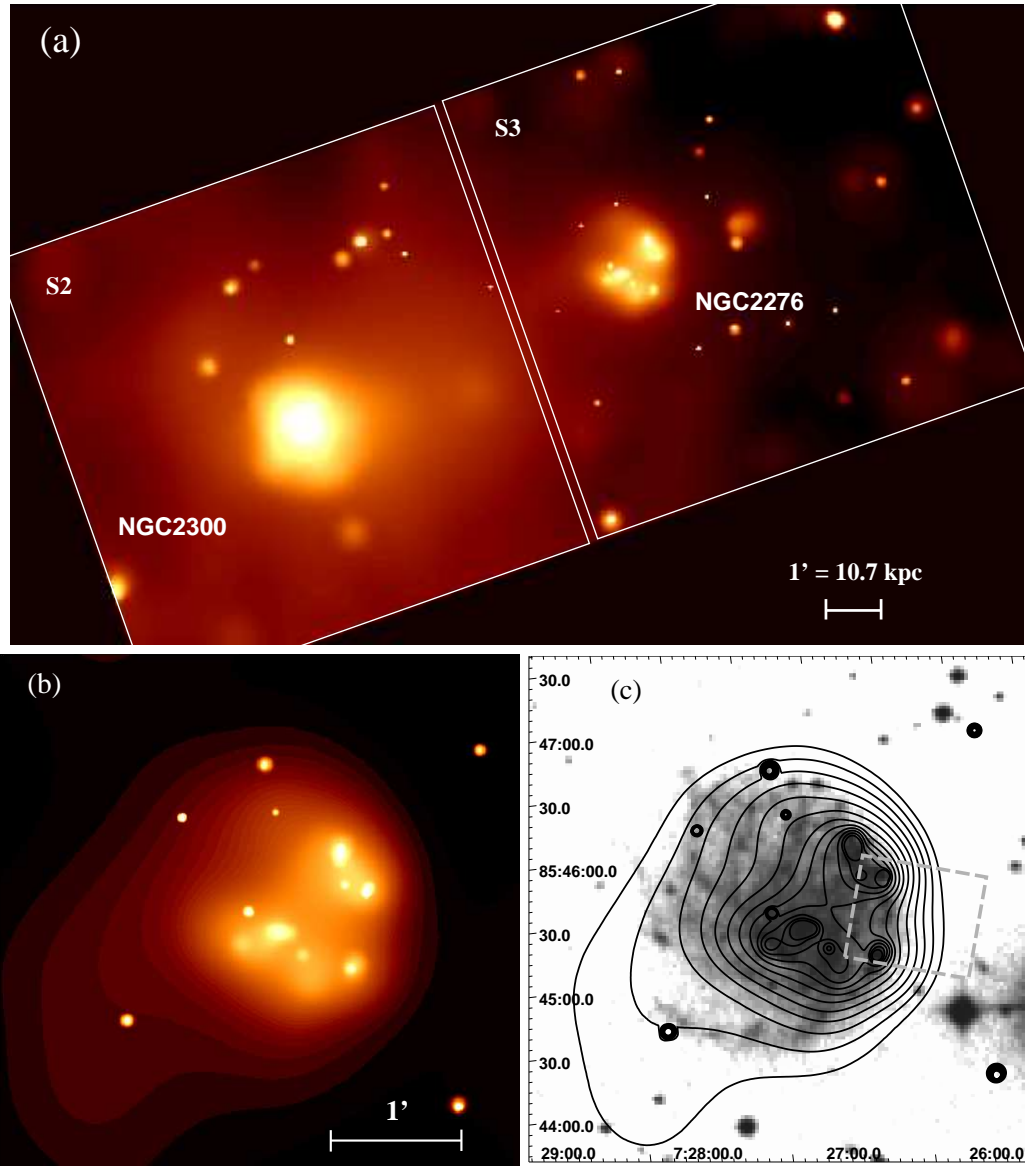


Figure 1. (a) 0.3–2 keV adaptively smoothed image of the full S2 and S3 CCDs (3σ – 5σ smoothing significance). (b) The central 4×4 arcmin² region surrounding NGC 2276. (c) Corresponding X-ray contours overlaid on a Digitized Sky Survey image. Dashed box shows the region used for extraction of surface brightness profiles across the western edge.

dom). We take the two-temperature model to be a representative parametrization of the integrated spectrum of diffuse emission. The total 0.3–2 keV luminosity of this emission is $L_X = 1.86 \pm 0.37 \times 10^{40}$ erg s⁻¹, and its spectrum and best-fitting model are shown in Fig. 4a. We tested whether the temperature derived for the hotter component was affected by residual emission from either low- or high-mass X-ray binaries, fixing this residual component to either a $\Gamma = 1.5$ power-law or a 7 keV thermal bremsstrahlung model (Irwin, Athey & Bregman 2003) for low-mass X-ray binaries, or a $\Gamma = 1$ power-law for high-mass ones (e.g. van der Meer et al. 2005). The best-fitting temperature for the hotter gas component is in all cases consistent with the value listed in Table 2, and the fitted models suggest that unresolved X-ray binary emission accounts for only 10–15 per cent of the total 0.3–2 keV flux. For the stellar mass

of NGC 2276 listed in Table 1, this emission level is consistent with the value of $L_X \approx 2 \times 10^{39}$ erg s⁻¹ expected for a population of low-mass X-ray binaries (Gilfanov 2004).

Spectra were also extracted for the east and west side of the disc separately (regions B and C in Fig. 2, selected so as to contain a similar number of net counts, ~ 750 in 0.3–5 keV). Fitting results are virtually identical for the two regions and are consistent with those derived for the X-ray bright W edge of the galaxy alone (region D). There is thus no spectral evidence that the hot gas in the W side of the disc is preferentially affected by external pressure and/or mixing with IGM gas arising from the galactic motion through the IGM.

We note that the low abundances derived for the disc gas could be misleading, due to the well-known Fe-bias, arising when fitting the spectrum of a multi-phase gas with a

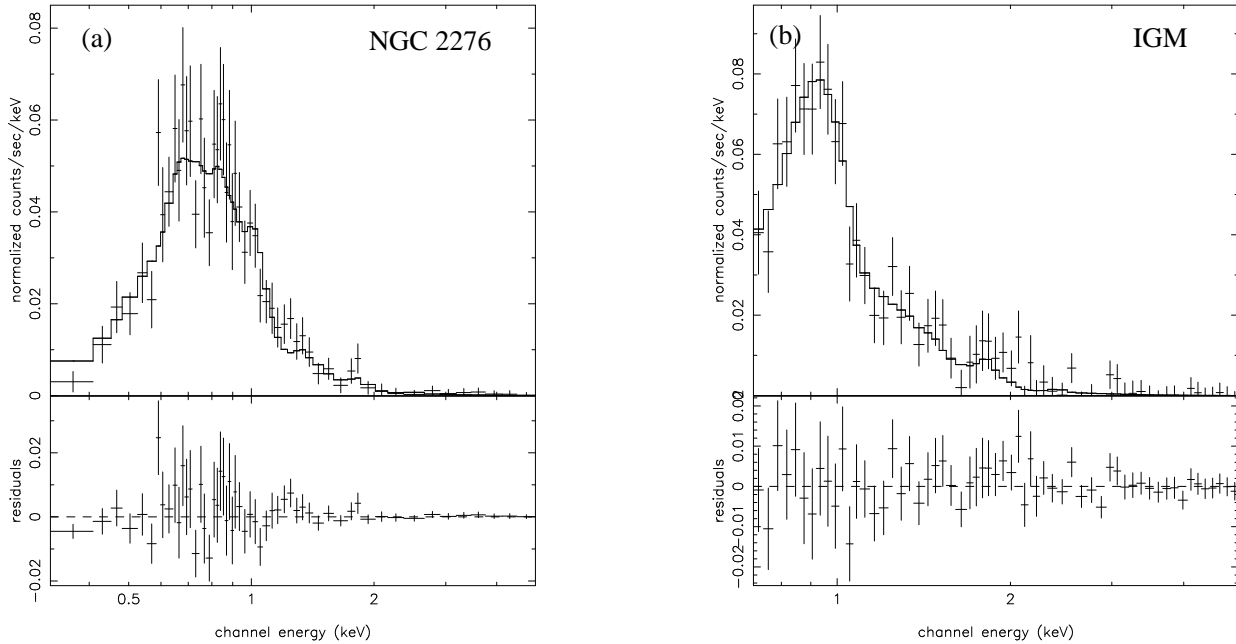


Figure 4. Spectrum and fitted model for (a) the NGC 2276 disc emission and (b) the surrounding IGM on the S3 chip. Bottom panels show fit residuals.

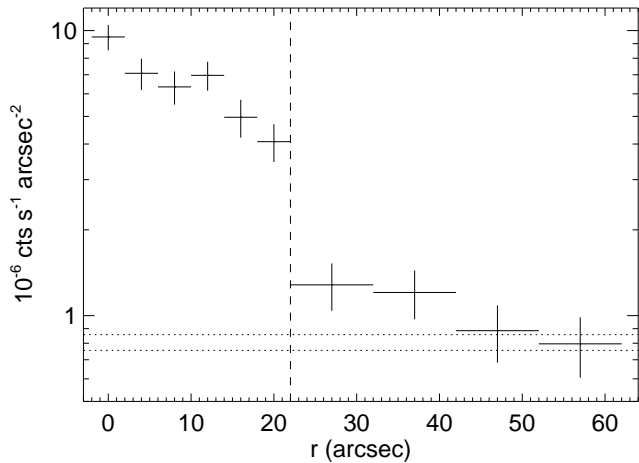


Figure 3. Exposure-corrected 0.3–2 keV surface brightness profile of diffuse emission across the western edge of the NGC 2276 disc. Dotted lines mark the 90 per cent confidence limits on the background level as determined from an on-chip background spectrum (i.e. including emission from the ambient IGM). Vertical dashed line marks the extent of the optical disc, quantified as D_{25} , the ellipse outlining a B -band isophotal level of $25 \text{ mag arcsec}^{-2}$.

single-temperature model (Buote 2000). For example, when allowing Z for the two-temperature model to vary, the result is consistent with supersolar abundances. This is testimony to the (anticipated) complexity of the spectrum, and the fitted models should be considered convenient means of parametrizing the disc spectrum rather than a complete description of the physical state of hot gas in the disc.

3.2 IGM

In order to validate the properties of the IGM emission as derived from earlier *ROSAT* studies, we modelled the 0.3–2 keV surface brightness distribution on the full S3 chip alone, using an elliptical β -model on top of a constant background, with NGC 2276 excised out to a radius of 1.5 arcmin. The appropriate exposure map was included in the fit, and the assumed peak of the emission was taken to be the position reported by Davis et al. (1996). We find $\beta = 0.41^{+0.06}_{-0.09}$, $r_c = 4.0 \pm 1.8$ arcmin, and $S_0 = 3.1 \pm 0.5 \times 10^{-3} \text{ counts s}^{-1} \text{ arcmin}^{-2}$, in excellent agreement with the *ROSAT* result of Davis et al. (1996) (when correcting S_0 for the difference in effective area). With a best-fitting eccentricity of $\epsilon = 0.28^{+0.12}_{-0.15}$ and a major axis position angle consistent with an east-west orientation, the derived large-scale morphology of the IGM emission is also qualitatively similar to the one found by Mulchaey et al. (1993) and Davis et al. (1996).

For the spectral analysis, source-free regions on the S2+S3 chips were defined, and spectra and responses were extracted separately for each chip. The spectra were fitted both individually for the two chips and jointly, with the spectrum from the S3 CCD and its best-fitting model shown in Fig. 4b. A joint fit yields $T = 0.85 \pm 0.04$ keV and $Z = 0.17^{+0.07}_{-0.05} Z_{\odot}$. The derived temperature is in good agreement with the value of $T = 0.97^{+0.11}_{-0.08}$ keV obtained by Davis et al. (1996) from three combined *ROSAT* PSPC exposures of the group. For comparison to this earlier study, we derive $Z = 0.11^{+0.04}_{-0.03} Z_{\odot}$ using the abundance table of Anders & Grevesse (1989). This is also consistent with the result of Davis et al. (1996), hence confirming the relatively low abundance of this group. The good agreement with the spatial and spectral results of Davis et al. (1996) implies that we can justifiably adopt their values for the peak IGM density and total IGM mass.

Table 2. Summary of spectral fits to diffuse emission in the 0.3–5 keV band (0.7–5 keV for the IGM fits, see text). Region labels are shown in Figs. 2 and 5 (‘S3\F’ means the S3 chip ‘excluding F’). Unabsorbed X-ray luminosities for the major components are presented in the 0.3–2 keV band. Last column gives the goodness of fit for the number of degrees of freedom ν .

Region	XSPEC model	Results (T/keV , Z/Z_{\odot})	L_X ($10^{39} \text{ erg s}^{-1}$)	χ^2/ν
NGC 2276 disc (A)	WABS(MEKAL)	$T = 0.53^{+0.08}_{-0.05}$, $Z = 0.10^{+0.04}_{-0.03}$...	58.9/52 (1.13)
...	WABS(MEKAL+POW)	$T = 0.34^{+0.04}_{-0.03}$, $Z = 2.11^{+25.29}_{-0.61}$, $\Gamma = 2.00^{+0.40}_{-0.20}$...	45.4/50 (0.91)
...	WABS(MEKAL+MEKAL)	$T_1 = 0.32^{+0.03}_{-0.03}$, $T_2 = 1.30^{+1.47}_{-0.35}$, $Z = 0.43^{+0.82}_{-0.16}$	18.6 ± 3.7	41.4/50 (0.83)
NGC 2276 E disc (B)	WABS(MEKAL)	$T = 0.51^{+0.11}_{-0.09}$, $Z = 0.06^{+0.04}_{-0.03}$	10.0 ± 2.9	26.9/28 (0.96)
NGC 2276 W disc (C)	WABS(MEKAL)	$T = 0.53^{+0.09}_{-0.08}$, $Z = 0.11^{+0.08}_{-0.05}$	9.1 ± 3.0	18.1/25 (0.72)
NGC 2276 W edge (D)	WABS(MEKAL)	$T = 0.55^{+0.07}_{-0.07}$, $Z = 0.11^{+0.08}_{-0.04}$	13.3 ± 4.0	24.7/24 (1.03)
NGC 2276 “tail” (E)	WABS(MEKAL)	$T = 0.84^{+0.35}_{-0.22}$, $Z = 0.17$ (fixed)	1.9 ± 0.5	0.3/3 (0.11)
...	WABS(MEKAL)	$T = 0.76^{+0.20}_{-0.18}$, $Z = 1.0$ (fixed)	...	0.9/3 (0.30)
IGM, S2 chip	WABS(MEKAL)	$T = 0.95^{+0.07}_{-0.09}$, $Z = 0.27^{+0.19}_{-0.13}$	41.7 ± 14.6	29.9/46 (0.65)
IGM, S3 chip (S3\F)	WABS(MEKAL)	$T = 0.81^{+0.05}_{-0.06}$, $Z = 0.17^{+0.13}_{-0.07}$	29.5 ± 9.8	41.5/76 (0.55)
IGM, S2+S3	WABS(MEKAL)	$T = 0.85^{+0.04}_{-0.04}$, $Z = 0.17^{+0.07}_{-0.05}$	70.3 ± 14.1	128.1/123 (1.04)
Shocked IGM (G)	WABS(MEKAL)	$T = 1.08^{+0.70}_{-0.33}$, $Z = 0.17$ (fixed)	...	0.4/3 (0.14)
Mach cone (H)	WABS(MEKAL)	$T = 1.06^{+0.32}_{-0.19}$, $Z = 0.17$ (fixed)	...	8.1/13 (0.73)
Mach cone (G+H)	WABS(MEKAL)	$T = 1.20 \pm 0.27$, $Z = 0.17$ (fixed)	...	8.9/15 (0.59)
Unshocked IGM (I)	WABS(MEKAL)	$T = 0.78 \pm 0.10$, $Z = 0.17$ (fixed)	...	38.6/37 (1.04)

4 DISCUSSION

The compression of the X-ray isophotes along the west edge of NGC 2276 and the presence of a tail of gas extending towards the east suggest that the hot gas morphology of the galaxy could be affected by its motion through the IGM. However, given the position of NGC 2300 and hence the IGM peak, it seems worthwhile first to establish to what extent the appearance of the eastern tail is distorted by superposition on the broader IGM surface brightness gradient. To investigate this, we smoothed the derived 2-D IGM model using the same spatial scales as used for producing Fig. 1, and subtracted it from the latter. The result, presented in Fig. 5, shows that the X-ray tail persists, still showing an overall morphology in line with the expectation if the gas distribution of the galaxy is affected by ram pressure caused by motion towards the west. Also shown in Fig. 5 are contours outlining the radio continuum emission in the galaxy (Davis et al. 1997), indicating the presence of a radio tail coincident with that seen in X-rays. We will now proceed to investigate whether the overall X-ray and radio morphologies could indeed be indicative of the direction of motion of NGC 2276 in the plane of the sky.

4.1 Velocity of NGC 2276 through the IGM

The distance from the IGM centre to the W edge of NGC 2276 is ~ 70 kpc. The gas mass and β -profile parameters derived by Davis et al. (1996) imply an IGM density outside the W edge of $n_e = 6 \pm 0.6 \times 10^{-4} \text{ cm}^{-3}$. Using $T_{\text{IGM}} \approx 0.81 \text{ keV}$ from Table 2, this then implies a thermal IGM pressure of $P_{\text{IGM}} \approx 1.6 \times 10^{-12} \text{ dyn cm}^{-2}$ outside this edge, and a local sound speed $v_s \approx 500 \text{ km s}^{-1}$.

The radial velocity difference Δv_r between NGC 2276 and NGC 2300, the two most massive group galaxies, is $\Delta v_r \approx 420 \text{ km s}^{-1}$ (Table 1). The more massive elliptical NGC 2300 is close to the IGM centre, so Δv_r should be a reasonable measure of the radial velocity of NGC 2276 relative to the ambient IGM, showing that the true 3-D speed

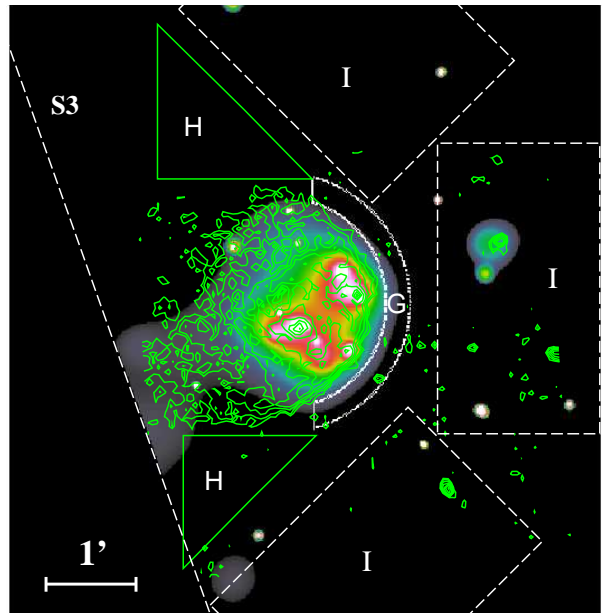


Figure 5. As Fig. 1, but for a 7×7 arcmin region around NGC 2276 and with IGM emission subtracted. Also shown are the regions (G+H) outside the W edge and inside the Mach cone used to search for evidence of shock-heating of the IGM (see Section 4.1 for details), with dashed regions (I) used for comparison spectra. Overlaid are Very Large Array 1.49 GHz contours from the data presented by Davis et al. (1997), starting at $0.05 \text{ mJy beam}^{-1}$ and spaced by a factor $\sqrt{2}$.

of this galaxy could easily be supersonic. In the absence of magnetic fields and assuming that radiative cooling of post-shock gas can be neglected (this will be justified below), the Rankine-Hugoniot shock adiabat for a one-dimensional shock would then imply

$$\frac{n_2}{n_1} = \frac{\gamma + 1}{\gamma - 1 + 2/M_1^2}, \quad (1)$$

$$\frac{T_2}{T_1} = \frac{(1 - \gamma + 2\gamma M_1^2)(\gamma - 1 + 2/M_1^2)}{(1 + \gamma)^2}, \quad (2)$$

for the density and temperature ratios of upstream (subscript 1) and downstream (subscript 2) gas¹. Here M_1 is the Mach number of the galaxy's motion through the IGM, and γ is the adiabatic index. Note that equation (1) implies a maximum density jump of $n_2/n_1 = 4$ for a shocked $\gamma = 5/3$ gas. Also note that both equations are strictly only valid for the region immediately in front of the galaxy, where the gas velocity can be taken to be perpendicular to the shock surface. For regions along the shock front further away from the shock symmetry axis, the gas will encounter an oblique shock wave, inclined by an angle $\phi < 90^\circ$ with respect to the galaxy velocity vector. In this case M_1 should be replaced by $M_1 \sin \phi$ in equations (1) and (2) (see, e.g., chapter 9 in Landau & Lifshitz 1987).

Is the diffuse X-ray emission from the W edge itself arising from a (shock)-compressed gas component? A low metal abundance is found for gas in the W disc, consistent with the value derived for the ambient IGM. This could point towards gas in the W disc being compressed IGM material rather than, e.g., starburst generated gas, but the Fe bias could be important here, as the full-disc spectral fits indicate the presence of at least two gas phases. If assuming a face-on disc (Gruendl et al. 1993 constrain the inclination to $9^\circ < i < 17^\circ$) of thickness 2 kpc, the derived spectrum and flux of 5.9×10^{-14} erg cm⁻² s⁻¹ imply a mean electron density of $n_e \approx 0.018$ cm⁻³, a thermal pressure of $P_{\text{th}} \sim 2n_e T \approx 3.1 \times 10^{-11}$ dyn cm⁻², and a gas mass of $M \approx 1.5 \times 10^8 M_\odot$ for the western half of the disc. The corresponding values for the east disc are very similar, implying a total hot gas mass of $M \approx 3.7 \times 10^8 M_\odot$ and no large-scale hot gas flows inside the disc due to pressure imbalances. Adopting the single-temperature model of the disc emission, the lower T relative to the IGM value suggests that this emission is not dominated by a *shocked* IGM. The density jump between IGM and disc gas of a factor ~ 30 is also much larger than can be achieved in a non-radiative shock, thus reinforcing this conclusion. As the temperature of the disc gas is typical of that inferred for starburst galaxies and since, for that temperature, both the X-ray luminosity and mass of this gas fall right on to the trends derived for starburst galaxies (Read & Ponman 2001), emission inside the W edge is most likely dominated by that of starburst-generated gas, although some mixing with the ambient IGM may have taken place.

Fig. 1c suggests evidence of X-ray emission beyond the optical W edge of NGC 2276. This component appears spatially distinct from the hot interstellar medium (cf. Fig. 3), and could arise predominantly from a compressed or even shocked IGM. A spectral fit to the emission immediately outside the W optical edge (region G in Fig. 5, corresponding to the two bins with excess emission in Fig. 3), gives $T = 1.08^{+0.70}_{-0.33}$ keV (for Z fixed at the global IGM value of $0.17 Z_\odot$ derived for the S3 chip; best-fitting value is $\sim 0.5 Z_\odot$ but statistics are too poor to obtain useful constraints on this quantity and neither the best-fitting T nor

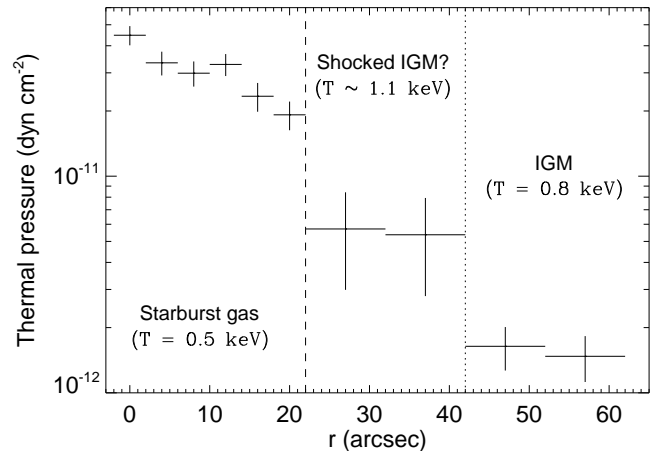


Figure 6. NGC 2276 pressure profile across the W edge.

its errors are very sensitive to changes in the assumed Z). Although nominally higher, this temperature is still consistent with that of the ambient IGM, but is inconsistent with the single-component value for the interstellar medium (ISM) in the disc. Moreover, comparing blank-sky and on-chip background levels suggests that only one-third of this emission is from fore-/background IGM. Motivated by this, we plot in Fig. 6 the thermal pressure corresponding to the surface brightness plot shown in Fig. 3, assuming that most of this emission immediately outside the W edge arises within a line-of-sight depth of $\lesssim 20$ kpc ($\approx 2r_D$, where r_D is the disc radius). Intriguingly, there is evidence for a build-up of pressure immediately outside the optical disc, consistent with a scenario in which the IGM in front of the galaxy is being pressurized due to the motion of the galaxy. For the assumed 20 kpc depth, we find a local mean density of $n_e \approx 1.6 \pm 0.7 \times 10^{-3}$ cm⁻³ and a pressure $P_{\text{th}} \approx 4.8 \times 10^{-12}$ dyn cm⁻² in this region. This suggests a density jump of a factor $n_2/n_1 = 2.6 \pm 1.2$ with respect to the ambient IGM, indicating a shock, but a corresponding jump in T cannot be unambiguously established from these results alone.

If a shock front is present, gas immediately inside the Mach cone will be affected also at some distance from NGC 2276. The asymptotic Mach angle α (the cone opening angle with respect to the symmetry axis) should satisfy $\sin \alpha = M_1^{-1}$. An initial guess of $\alpha \approx 40\text{--}45^\circ$, based on the X-ray and optical morphology of the W edge, would correspond to a mild shock of Mach number $M_1 \approx 1.5$. To help constrain the temperature of gas inside this potential shock front, we also considered regions outside the optical disc but immediately inside the $M_1 \approx 1.5$ Mach cone (regions H in Fig. 5). Despite the fact that these regions are further away from the shock symmetry axis than the W edge and so should experience a smaller temperature jump (as mentioned above, due to M_1 in equation 2 being replaced by $M_1 \sin \phi$, where $\alpha < \phi < \pi/2$), we find $T = 1.06^{+0.32}_{-0.19}$ keV, which is still marginally inconsistent with the unshocked IGM value. In an attempt to maximize the S/N ratio and obtain tighter constraints on the post-shock temperature, we performed a joint fit to the emission in these regions

¹ As is customary in the literature, we use subscripts 1 and 2 to distinguish upstream from downstream quantities throughout this paper.

and that of the W edge (i.e. regions G+H in Fig. 5). We readily acknowledge the fact that T is not expected to be uniformly raised across this region, but the result is expected to be dominated by statistical errors anyway. This approach gives $T = 1.20 \pm 0.27$ keV, thus strengthening the inconsistency with the local IGM value. The temperature jump between the putative shocked and unshocked regions is then $T_2/T_1 = 1.48 \pm 0.28$, in agreement with the expectation from equation (2) for an $M_1 \approx 1.5$ shock. For the derived density jump of $n_2/n_1 = 2.6 \pm 1.2$, this result is also in formal agreement with the maximum ratio $T_2/T_1 = 2.6_{-1.3}^{+3.8}$ predicted by equations (1) and (2) for $\phi = 90^\circ$. As a consistency check, we confirmed that the emission level in various regions upstream of the $M_1 \approx 1.5$ Mach cone (regions I) is consistent with that of the (background plus) local IGM, rendering it unlikely that our results for the two regions inside the Mach cone are substantially affected by inaccurate background subtraction.

One would also expect an increase in surface brightness across the edges of the Mach cone, but such a jump is not convincingly detected. However, this could be due to geometrical effects. In particular, we suffer from not knowing the exact 3-D direction of motion of NGC 2276 and the resulting orientation of the Mach cone, which makes it non-trivial to provide a meaningful surface brightness plot for the Mach cone corresponding to that presented in Fig. 3. Also, when projected on to the sky, the surface brightness will be continuous at a shock even though the gas density is discontinuous at the front, because shock fronts are invariably curved. Projection effects will therefore tend to smear out any sharp increase in the X-ray emission across the front. Nevertheless, even after subtracting the best-fitting IGM surface brightness model from the data, we do detect a clear enhancement in surface brightness inside the Mach cone (regions H in Fig. 5), which is found to be ~ 80 per cent higher than in regions immediately outside this cone (regions I). There is a corresponding jump in T , measured to be $T = 0.78 \pm 0.10$ keV in regions I, compared to the 1.20 ± 0.27 keV inside the Mach cone.

The data are thus consistent with a mildly shocked IGM. The density jump observed across the W edge, and the temperature jump in this and the Mach cone regions, translate, via equations (1) and (2), into consistent Mach numbers $M_1 = 2.4_{-1.1}^{+1.8}$ and $M_1 = 1.5 \pm 0.3$, respectively. Combining the information on density and temperature, one can evaluate the shock (and hence galaxy) speed directly as (see e.g. Henry, Finoguenov & Briel 2004)

$$v_{\text{gal}} = \frac{1}{1 - n_1/n_2} \left[\frac{kT_1}{\mu m_p} \left(\frac{n_2}{n_1} - 1 \right) \left(\frac{T_2}{T_1} - \frac{n_1}{n_2} \right) \right]^{1/2}, \quad (3)$$

yielding $v_{\text{gal}} = 784 \pm 103$ km s $^{-1}$. The derived error on v_{gal} is the dispersion resulting from 10,000 Monte Carlo realizations of equation (3), for which parameters were drawn from a Gaussian distribution centred at their best-fitting values and having σ equal to the measured 1σ uncertainty. Nominally, the result implies a Mach number $M_1 = 1.54 \pm 0.20$.

However, several effects tend to make the measured value of the temperature jump smaller than it would be in a simple, normal shock at the velocity of the galaxy. First, emission from unshocked gas projected into the line-of-sight could reduce the measured temperature of the shocked gas.

We have attempted to reduce the impact of this effect by using on-chip background estimates from unshocked regions (see Fig. 2). Second, in region G in Fig. 5, the shock strength should vary quite significantly, since, as mentioned above, the effective Mach number varies as $\sin \phi$, where ϕ is the angle between the galaxy velocity vector and the shock front. Thirdly, for the same reasons, the shock is almost certainly weaker for region H than in region G. The fact that we can even detect a temperature excess in region H almost certainly requires that the galaxy is moving considerably faster than our simple estimate. Fourthly, the postshock pressure returns quickly to the ambient gas pressure in the downstream flow. Most of the gas begins to expand adiabatically and cool immediately behind the shock (gas close to the stagnation point at the leading edge of the galaxy is the exception). In combination, these effects will generally reduce the measured temperature jump. The derived jump will therefore almost certainly underestimate the true Mach number of the galaxy relative to the IGM.

In addition, the actual Mach number is further underestimated due to projection effects. Given a line-of-sight velocity Δv_r of NGC 2276 relative to the group, a sound speed v_s , and the apparent (i.e. measured) opening angle α of the Mach cone projected on to the sky, the intrinsic Mach number \mathcal{M} is given by

$$\mathcal{M} = \frac{[1 + (\Delta v_r \sin \alpha)^2 / v_s^2]^{1/2}}{\sin \alpha}. \quad (4)$$

Using $\Delta v_r \approx 420$ km s $^{-1}$ and $\alpha \approx 40\text{--}45^\circ$, this corresponds to $\mathcal{M} \approx 1.7$. If adopting the fractional errors derived for equation (3) and adding these in quadrature to those resulting from varying α within the range $40\text{--}45^\circ$, one finds $\mathcal{M} = 1.70 \pm 0.23$, i.e. a pre-shock velocity of $v_1 = 865 \pm 120$ km s $^{-1}$ of the galaxy relative to the IGM. We note, for the various reasons mentioned above, that the actual speed of the galaxy could be even higher, although this is not easily quantified and may well be subsumed by the large uncertainties. For the purposes of this paper, which is to investigate the importance of ram pressure, the 'deprojected' Mach number of $\mathcal{M} \approx 1.7$ should be a conservative choice which we will consequently adhere to in the following. The implied density and temperature jumps from equations (1) and (2) are then $n_2/n_1 = 2.0$ and $T_2/T_1 = 1.7$, respectively.

4.2 The effects of ram pressure

Assuming a shock is present, conservation of the mass flux density $\rho_{\text{ICM}} v_{\text{gal}}$ perpendicular to the shock front implies that the true ram pressure felt by the galaxy will be smaller than that upstream of the front. For $\mathcal{M} = 1.7$, the implied density increase of a factor 2.0 corresponds to a decrease in galaxy-IGM velocity to $v_{\text{gal}} \approx 430$ km s $^{-1}$. This is thus the velocity v_2 of post-shock gas immediately behind the shock front. We note that the cooling time of this gas is ~ 14 Gyr, thus justifying the non-radiative assumption underlying equations (1) and (2). The resulting ram pressure $P_{\text{ram}} = \rho_{\text{ICM}} v_{\text{gal}}^2 = \rho_2 v_2^2 \approx 3.7 \times 10^{-12}$ dyn cm $^{-2}$, which, combined with the increased thermal IGM pressure behind the shock front, yields a total IGM pressure $P_{\text{tot}} = P_{\text{ram}} + P_{\text{th}} \sim 9 \times 10^{-12}$ dyn cm $^{-2}$. This is a factor of 3 less than the mean thermal pressure of the hot ISM in

the disc, at first suggesting that the morphology of hot disc gas would be only marginally affected by ram pressure.

However, a more detailed treatment of the effects of ram pressure, in particular the question of ram-pressure *stripping*, must take into account two additional considerations. One is the gravitational restoring force per unit area of the disc (Gunn & Gott 1972), $F/A = 2\pi G\Sigma_*\Sigma_g$, where Σ_* and Σ_g are the surface densities of stars and gas, respectively. The classical condition for ram-pressure stripping to occur then becomes $\rho_{\text{ICM}}v_{\text{gal}}^2 > 2\pi G\Sigma_*\Sigma_g$, i.e.

$$\left(\frac{n_e}{\text{cm}^{-3}}\right)\left(\frac{v_{\text{gal}}}{\text{km/s}}\right)^2 \gtrsim 100\left(\frac{M_*}{M_\odot}\right)\left(\frac{M_g}{0.1M_*}\right)\left(\frac{r_{\text{D}}}{\text{kpc}}\right)^{-4}, \quad (5)$$

where n_e is the IGM electron density, r_{D} the disc radius, and M_* and M_g is the mass of stars and gas in the disc, respectively. The validity of this estimate has been supported by results of numerical simulations (Abadi et al. 1999). The other issue to consider is that while the ram pressure itself is reduced at the shock, $P_{\text{th}} + \rho v^2$ remains conserved (for an inviscid fluid). Thus, the reduction in ram pressure behind the shock front is balanced by an increase in static (thermal) pressure. Now, the difference between the static pressure at the stagnation point, where the flow meets the leading edge of the galaxy, and the upstream thermal pressure is approximately equal to the upstream ram pressure. As long as the galactic disc remains intact (and the effective Reynolds number is reasonably high), a region of separated flow can be expected behind the disc, where the pressure is approximately equal to the downstream (i.e. ambient) gas pressure. The quantity relevant to the issue of ram pressure stripping, the force per unit area acting on a disc normal to the flow, is thus close to the pre-shock ram pressure.

Using therefore the pre-shock values of $n_e = n_1 = 6 \times 10^{-4} \text{ cm}^{-3}$ and $v_{\text{gal}} = v_1 = 865 \text{ km s}^{-1}$ in equation (5), along with M_* from Table 1, $r_{\text{D}} = 10 \text{ kpc}$, and $M_g = 6.4 \times 10^9 M_\odot$ (Young et al. 1989), one finds a ram-pressure falling short of F/A by a factor ~ 15 . The central IGM density is only a factor 1.7 larger than the value assumed, so using this value instead does not change the immediate conclusion that ram pressure stripping should not have been an important factor in the recent evolution of NGC 2276. Moreover, the assumed value of n_e could be optimistic, as NGC 2276 could be further away from the IGM centre than indicated by the projected distance. However, the velocity dispersion of the group is $\sigma \approx 300 \text{ km s}^{-1}$ (Mulchaey et al. 1993), in excellent agreement with the expectation from the σ - T relation for X-ray bright groups (Osmond & Ponman 2004). The larger values of both Δv_r and v_{gal} may suggest that NGC 2276 is currently passing through the group core, so we are probably not making a large error in taking the projected distance to NGC 2300 as representative of the true distance to the IGM density peak.

An important caveat associated with the stripping criterion of equation (5) is that the gas is assumed to be held in place by a homogeneous disc thin enough to be described solely by its surface density Σ . In order to provide a more realistic picture of the effects of ram pressure, the calculation should be repeated as a function of radius R in the disc midplane, and vertical disc height $|z|$, under suitable assumptions about the distribution of gas, stars, and dark matter (DM). For this purpose, we set up a model of the

Table 3. Adopted parameters of the galaxy model. L is the characteristic scalelength for each component, i.e. r_{h} and r_{t} for the halo, r_{b} for the bulge, and R_{d} and z_{d} for the disc components.

Component	M_{total} ($10^{10} M_\odot$)	L (kpc)
DM halo	8.00	3.5, 30
Stellar bulge	0.55	0.3
Stellar disc	2.15	3.0, 0.25
Cold gas disc	0.64	2.5, 0.25
Hot gas disc	0.04	3.0, 1.0

gravitational potential $\Phi(R, z)$ of NGC 2276. We adopted the model of Abadi et al. (1999) which consists of a spherical bulge with density profile

$$\rho_{\text{b}}(r) = \frac{M_{\text{b}}}{2\pi r_{\text{b}}^2} \frac{1}{r(1+r/r_{\text{b}})^3}, \quad (6)$$

a spherical DM halo,

$$\rho_{\text{h}}(r) = \frac{M_{\text{h}}}{2\pi^{3/2}} \frac{\eta}{r_{\text{t}} r_{\text{h}}^2} \frac{\exp(-r^2/r_{\text{t}}^2)}{(1+r^2/r_{\text{h}}^2)}, \quad (7)$$

and exponential stellar and gaseous discs, each of the form

$$\rho_{\text{d}}(R, z) = \frac{M_{\text{d}}}{4\pi R_{\text{d}}^2 z_{\text{d}}} \exp(-R/R_{\text{d}}) \text{sech}^2(z/z_{\text{d}}). \quad (8)$$

Here M_{b} , M_{h} , and M_{d} are the total masses of each component, r_{b} and r_{h} are the scalelengths of the bulge and halo, respectively, r_{t} is the halo truncation radius, R_{d} is the cylindrical scalelength of the disc components and z_{d} the corresponding thickness, and finally

$$\eta = \{1 - \pi^{1/2} q \exp(q^2) [1 - \text{erf}(q)]\}^{-1}, \quad (9)$$

where $q = r_{\text{h}}/r_{\text{t}}$ and erf is the error function. We adopt again the stellar mass M_* from Table 1, a cold gas mass $M_{\text{g}} = 6.4 \times 10^9 M_\odot$, a hot X-ray emitting gas mass $M_{\text{hot}} = 3.7 \times 10^8 M_\odot$ (cf. Section 4.1), and a bulge-to-disc stellar mass ratio of 0.25, appropriate for an Sc spiral like NGC 2276. In order to comply with the observed size of the disc, the scalelength for the disc components have been fixed by the requirement that 90 per cent of all gaseous and stellar mass should lie within $r_{\text{D}} \approx 10 \text{ kpc}$. A vertical scaleheight of 1 kpc was adopted for the X-ray emitting component, representative of the values derived for galaxies of the mass and size of NGC 2276 in the disc galaxy sample of Strickland et al. (2004). The mass and truncation radius of the DM halo are then set by the requirement that the maximum disc circular velocity v_{rot} be within the observed limits of $v_{\text{rot}} \approx 120_{-40}^{+55} \text{ km s}^{-1}$ (mean value from the HyperLeda database). The adopted model parameters are listed in Table 3, and Fig. 7 illustrates the contribution of the various model components to the rotational disc velocity; the adopted model has a maximum rotational velocity of $v_{\text{rot}} \approx 140 \text{ km s}^{-1}$ at $r \approx 7 \text{ kpc}$, consistent with observations.

The restoring gravitational acceleration $\frac{\partial \Phi}{\partial z}(R, z)$ in the direction z perpendicular to the disc can be evaluated analytically for each model component using the equations of Abadi et al. (1999), to whom we refer for more details. Also, the values of Δv_r and (the pre-shock) $v_{\text{gal}} = v_1$ for NGC 2276 imply motion at an angle $\xi \approx 29^\circ$ with respect

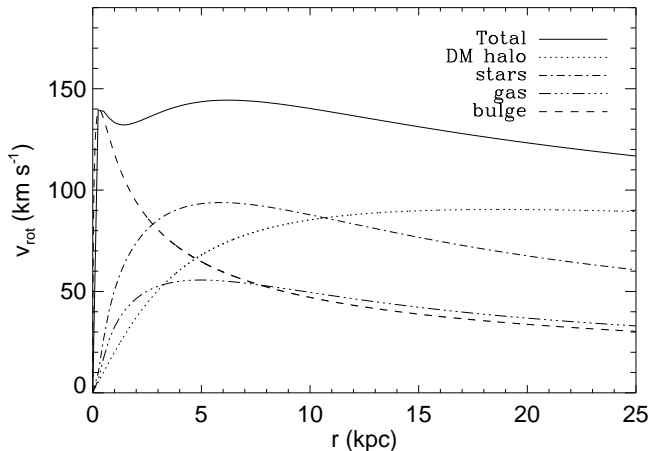


Figure 7. Contribution to the rotational disc velocity from the different components of the galaxy model.

to the plane of the sky. Given the small inclination under which the galaxy is viewed, this implies a reduction in the nominal ram pressure felt by the disc by a factor ≈ 4 relative to a situation where the disc is experiencing a face-on encounter with the IGM. The condition for ram-pressure stripping now becomes

$$\Sigma_g \left(\frac{\partial \Phi_b}{\partial z} + \frac{\partial \Phi_h}{\partial z} + \frac{\partial \Phi_g}{\partial z} + \frac{\partial \Phi_*}{\partial z} \right) < \rho_1 (v_1 \sin \xi)^2. \quad (10)$$

In Fig. 8, we plot the left-hand side of equation (10) along with the derived ram pressure. As was also found by Roediger & Hensler (2005) for their galaxy models, the gravitational restoring force in the outer disc ($R \gtrsim 5$ kpc) is seen to be nearly independent of z for all interesting values of this parameter. The figure suggests that at present, ram pressure alone is probably not powerful enough to remove large amounts of cold disc gas. But it also shows that the inferred stripping radius, outside which $P_{\text{ram}} > F/A$, is close to 10 kpc for the adopted galaxy model, in excellent agreement with the observed truncation radius of cold and hot gas along the W edge of NGC 2276. Ram pressure could therefore have played an important role in establishing the present size of the gas disc.

Fig. 8 further illustrates the region outside which P_{ram} exceeds the thermal pressure of the cold ($T \lesssim 10^4$ K) ISM not immediately affected by star formation. Outside this region, one would expect the distribution of cold gas, such as the $\text{H}\alpha$ emitting disc gas, to be significantly modified by ram pressure. Regarding the hot X-ray emitting ISM, P_{ram} exceeds the thermal pressure of this gas at heights $|z| \gtrsim 1$ –2 kpc above the disc. Starburst outflows would therefore be strongly affected by ram pressure and could be swept away before having time to fall back on to the disc. Furthermore, if the X-ray emitting disc gas is mainly generated in stellar outflows, its distribution would at least initially follow that of young stars and hence that of the HI out of which these stars are formed (recall that the HI distribution is also compressed along the W edge). Such outflows will expand along the steepest density gradient, which will be perpendicular to the disc and thus close to a direction along the line of sight.

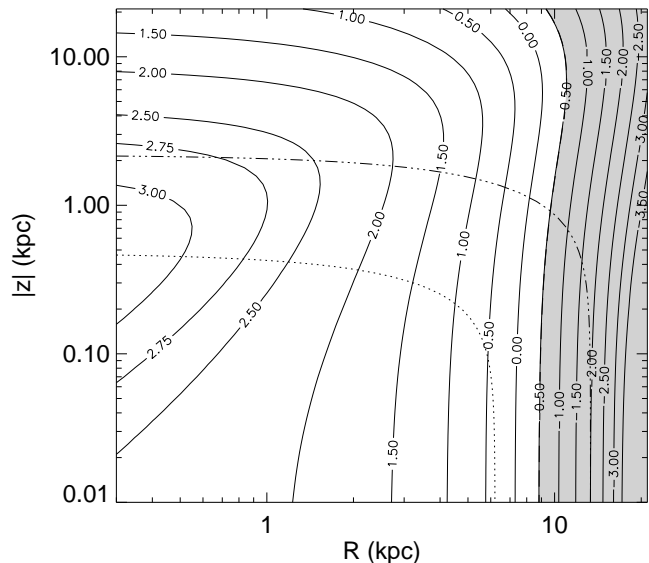


Figure 8. Logarithmic isocontours of the gravitational restoring force F/A perpendicular to the disc, in units of $10^{10} M_{\odot} \text{ kpc}^{-3} (\text{km s}^{-1})^2$. The shaded area outlines the region where galactic gas can be stripped by the derived ram pressure, $\log P_{\text{ram}} \simeq -0.5$. Dotted and dash-dotted lines mark the regions outside which P_{ram} exceeds the thermal pressure of cold and hot disc gas, respectively.

When viewed in projection, the X-ray emission from stellar outflows may therefore retain the apparent compression along the W edge both at early and late outflow stages.

It is instructive to also consider the effects of ram pressure on the hot coronal gas believed to surround at least massive ($v_{\text{rot}} \gtrsim 120 \text{ km s}^{-1}$) spiral galaxies at low redshift (White & Frenk 1991; Toft et al. 2002; Birnboim & Dekel 2003). This gas is assumed to provide the reservoir from which large disc galaxies are continuously replenishing the disc gas consumed in star formation, and is essential to explaining the extended star formation histories of isolated disc galaxies like the Milky Way. For a galaxy similar to NGC 2276, this gas component is expected to have $T \lesssim 0.1$ keV and $L_X \lesssim 10^{38} \text{ erg s}^{-1}$ (Toft et al. 2002; Rasmussen et al. 2006) and so would not be detectable in the present data. With an expected warm/hot gas mass of $\sim 10^8 M_{\odot}$ outside the disc (Rasmussen et al. 2006), the mean thermal pressure of this gas will be $P \lesssim 3 \times 10^{-13} \text{ dyn cm}^{-2}$ for a spherical corona of radius $r_D \approx 10$ kpc ($\log P \lesssim -1.35$ in the units of Fig. 8). While Fig. 8 indicates that a considerable fraction of this gas would remain bound in the galactic gravitational potential, ram pressure should disrupt its gradual inflow in this potential, preventing it from attaining the densities necessary for rapid cool-out on to the disc (see Acreman et al. 2003). Effectively, this will eventually halt star formation in the disc in a scenario identical to strangulation, but there is currently sufficient gas in the NGC 2276 disc for star formation to proceed at its present rate for at least another Gyr.

Transport processes could be more efficient than ram-pressure in removing gas from the galaxy. The expected mass

loss rate due to viscous stripping via Kelvin-Helmholtz instabilities is $\dot{M}_{\text{KH}} \approx \pi r_{\text{D}}^2 \rho_{\text{ICM}} v_{\text{gal}}$ (Nulsen 1982), i.e.

$$\dot{M}_{\text{KH}} \approx 0.1 \left(\frac{n_e}{\text{cm}^{-3}} \right) \left(\frac{r_{\text{D}}}{\text{kpc}} \right)^2 \left(\frac{v_{\text{gal}}}{\text{km s}^{-1}} \right) M_{\odot} \text{ yr}^{-1}. \quad (11)$$

This would imply $\dot{M}_{\text{KH}} \approx 5 M_{\odot} \text{ yr}^{-1}$ for the disc of NGC 2276. Note that, because $\rho_{\text{ICM}} v_{\text{gal}}$ is conserved across the shock front, the expected efficiency of viscous stripping is unaffected by the presence of a shock front. The viscous stripping efficiency is also largely insensitive to the orientation of the galaxy with respect to the direction of motion (Nulsen 1982; Quilis et al. 2000), unlike that of ram pressure stripping.

The mass loss rate due to thermal conduction of heat from the IGM to the ISM, whereby the colder disc gas is heated above the escape temperature of the galaxy (only counteracted by radiative cooling), can be 3.5 times larger than \dot{M}_{KH} (Nulsen 1982). But the efficiency of this process is uncertain due to the strong magnetic fields present in the disc, as evidenced by the radio continuum emission (indicating a field strength roughly twice the average of spirals; Hummel & Beck 1995). The fact that the large majority of the ISM (~ 95 per cent) is in a cold phase suggests that conduction of heat from the IGM is not currently an important process.

In summary, these results indicate that shock compression can explain the presence of slightly denser and hotter gas outside the leading edge of galaxy, and that it could certainly exert a significant influence on the ISM, both in terms of establishing the size of the gas disc and compressing the HI and X-ray contours along the W edge, as well as helping to trigger the substantial star formation along this edge. In this context it is also interesting to note the optical result of Davis et al. (1997) that the radial gradient in $[\text{OIII}]/\text{H}\beta$ is twice as steep on the western side compared to the eastern side of the disc, a result which could be attributed to gas in the W disc being swept inward (potentially promoting the growth of a larger bulge). Starburst outflows would be swept back by ram pressure, and the cooling out of hot coronal gas on to the disc would be inhibited. Ram-pressure, however, is probably insufficient to strip large amounts of gas from the disc, whereas hydrodynamic instabilities arising along the ISM/IGM boundary could be removing ISM material from the galaxy at a rate of several solar masses per year.

4.3 The nature and origin of the X-ray tail

The presence of an X-ray tail extending eastwards from the disc of NGC 2276 is established at the 3σ significance level, based on the enhancement in surface brightness within this region relative to the on-chip background. While its presence is thus tentative rather than conclusive, the location of the tail matches that of a similar structure seen in both HI and radio continuum data (Hummel & Beck 1995; Davis et al. 1997). Only one clear-cut example of such an X-ray tail trailing a spiral in a poor group has so far been reported (Machacek et al. 2005a). The X-ray luminosity of the NGC 2276 tail is $\sim 2 \times 10^{39} \text{ erg s}^{-1}$, about 10 per cent of that of the diffuse disc gas. The tail is not seen in the optical; in particular, there is no evidence from H α data of ongoing star formation in this region (Gruendl et al. 1993).

A single X-ray point source is detected at $> 3\sigma$ significance in the tail, but statistics are too poor (~ 20 net counts) to allow a test of whether this is a background source.

The hot tail gas has a temperature $T \sim 0.8 \text{ keV}$, consistent with that of the surrounding IGM. Extending to a galactocentric distance of $\sim 20 \text{ kpc}$, the tail gas should be essentially unbound from the galaxy, for which the characteristic escape temperature at this position is $kT_{\text{esc}} = \mu m_p v_{\text{esc}}^2 / 3 \approx 0.1 \text{ keV}$ as derived from our galaxy model. If the tail line-of-sight depth is $\sim r_{\text{D}} \approx 10 \text{ kpc}$, and assuming $Z = 0.2 Z_{\odot}$, its density and hot gas mass are $n_e \sim 2.8 \times 10^{-3} \text{ cm}^{-3}$ and $\sim 1.2 \times 10^8 M_{\odot}$, respectively, with both these numbers reduced by roughly a factor 2 for a $Z = Z_{\odot}$ plasma. The galaxy moves a distance corresponding to the extent of the tail ($\sim 10 \text{ kpc}$ at $v_2 = 430 \text{ km s}^{-1}$) in $\sim 20 \text{ Myr}$. If the entire mass of the X-ray tail represents unbound gas displaced from the disc due to the motion of NGC 2276, this would imply a mass loss rate averaged over the disc of order $\dot{M}_{\text{tail}} \sim 3\text{--}6 M_{\odot} \text{ yr}^{-1}$. Of course, this relies on the assumption that the speed of the tail (relative to the galaxy) equals that of the shocked gas. However, as we will see, a significant fraction of tail gas is likely to represent hot disc gas which has been heated and accelerated by the shock, supporting this assumption.

For the HI tail, a rough estimate of its mass can be obtained from the HI map of Davis et al. (1997). Using $M_{\text{HI}} \approx 2.36 \times 10^5 (D/\text{Mpc})^2 (F_{\text{HI}}/\text{Jy})$ (where F_{HI} is the integrated HI flux in the tail; see, e.g., Rosenberg & Schneider 2002), we find $M_{\text{HI}} \sim 4 \times 10^7 M_{\odot}$. Taken at face value, this would correspond to a mass loss rate of $\sim 2 M_{\odot} \text{ yr}^{-1}$ of cold gas, assuming, as for the X-ray tail, that the galaxy has moved a distance corresponding to the extent of the tail in $\sim 20 \text{ Myr}$. The HI tail could therefore be accounted for by viscous stripping. However, our mass model of the galaxy suggests that this cold gas would remain bound in the potential of NGC 2276. As our main focus is the gas that can potentially be completely lost from the galaxy, we will concentrate on the origin of the X-ray tail in the following.

There appear to be at least four potential origins for this hot tail: gravitationally focused IGM material (a “wake”), gas stripped off by ram pressure or other transport processes, starburst-driven outflows being swept back by the same processes, or gas being tidally displaced by interaction with NGC 2300 and/or the group potential. A robust metallicity constraint could help distinguish between these scenarios, but the tail metallicity is essentially unconstrained. One immediately attractive explanation is that the tail results from viscous stripping, as the expected mass loss rate due to this mechanism is consistent with that inferred from the properties of the tail. It is nevertheless instructive to consider alternative explanations, so below we will discuss these different scenarios in more detail.

With spectral properties similar to those of the ambient IGM, the tail could be a wake of gravitationally focused IGM material. Although in analytical theory large-scale wakes are unlikely to be produced by galaxies moving supersonically (Sakelliou 2000), the simulation results of Stevens et al. (1999) indicate that wakes *can* be created behind supersonic (group) galaxies. If so, they should be most easily observable in a relatively cool ICM (Stevens et al. 1999; Sakelliou 2000). However, in order to produce an observable wake, the accretion radius for Bondi-Hoyle accretion must exceed

the galaxy radius (Sakelliou 2000) which translates into the requirement

$$M_{\text{gal}} \geq 8.7 \times 10^{11} \left(\frac{T}{\text{keV}} \right) \left(\frac{r_{\text{D}}}{10 \text{ kpc}} \right) M_{\odot} \quad (12)$$

for the total galaxy mass, i.e. $M_{\text{gal}} \gtrsim 8 \times 10^{11} M_{\odot}$ for the $r_{\text{D}} \approx 10$ kpc disc of NGC 2276. Given a stellar mass of $M_{*} \lesssim 3 \times 10^{10} M_{\odot}$ (Table 1), it seems unlikely this requirement can be met unless NGC 2276 is enveloped in an unusually massive dark matter halo. This can probably be ruled out by our rotation curve modelling, as the upper limit to v_{rot} of 175 km s^{-1} suggests $M_{\text{gal}} < 2.5 \times 10^{11} M_{\odot}$ for our adopted galaxy model. Another concern is that the tail gas is at least a factor of 2 denser than the surrounding IGM. For adiabatic accretion behind the galaxy, conservation of entropy, $S = T/\rho^{2/3}$, would then predict a corresponding temperature ratio of $T_{\text{tail}}/T_{\text{IGM}} \approx 1.6$, which is not favoured by the data. Consequently, while dedicated hydro-simulations would be necessary to assess the feasibility of this scenario in detail, we tentatively conclude that the tail is unlikely to be a wake.

Another explanation for the tail could be sought in a tidal interaction between NGC 2276 and NGC 2300. From the morphology of NGC 2276, Hummel & Beck (1995) estimate that the time t_{app} since closest approach between the galaxies is between half and one revolution of NGC 2276, about 3×10^8 yr. Assuming NGC 2300 is at rest within the group potential, a lower limit to t_{app} can be obtained from the tangential velocity $v_t = (v_{\text{gal}}^2 - \Delta v_r^2)^{1/2}$ of NGC 2276, which can be constrained to $v_t \lesssim 870 \text{ km s}^{-1}$, conservatively using our upper limit of $\mathcal{M} \approx 1.9$. This implies $t_{\text{app}} \gtrsim 80$ Myr for a projected distance of 75 kpc. Assuming an average galactocentric distance of $r \approx 15$ kpc, the dynamical time-scale for tail gas to recentre on NGC 2276 is $t = (2r^3/GM)^{1/2} \approx 160$ Myr as derived from our galaxy model. Since this is larger than t_{app} , the tail could potentially be the remnant of an interaction with NGC 2300. An argument against this, however, is the fact that the mass of hot gas in the tail constitutes ~ 15 – 25 per cent of all X-ray emitting gas in NGC 2276. If tidal interactions were responsible for the tail, then a similar fraction of stellar light should be deposited in a tidal tail. This is easily ruled out by optical observations. It is also curious that, if the tail is older than 80 Myr, it has not been wound up as a result of taking part in the overall differential rotation of the NGC 2276 disc. Given $v_{\text{rot}} \sim 120 \text{ km s}^{-1}$, the age constraint implies at least a quarter of a full revolution since the time of closest approach with NGC 2300. It is hard to see how the observed tail morphology could survive for so long.

A third possibility for the origin of the tail is related to the star formation rate of NGC 2276 of ~ 2 – $5 M_{\odot} \text{ yr}^{-1}$, as estimated from the relations of Kennicutt (1998) using either the $\text{H}\alpha$ flux of Davis et al. (1997), or the far-infrared luminosity (calculated from *IRAS* 60 and 100 μm fluxes). Hence, the tail could represent gas lost in starburst outflows which have subsequently been swept back by ram pressure. Given the inclination of the galaxy, the presence of such outflows cannot be directly inferred from the present data. However, in the disc galaxy sample of Strickland et al. (2004), all galaxies having a surface supernova (SN) rate above $40 \text{ Myr}^{-1} \text{ kpc}^{-2}$ also exhibit significant extraplanar X-ray emission, presumably resulting from starburst outflows. Us-

ing the same approach as Strickland et al. (2004), we find a corresponding SN rate of $280 \text{ Myr}^{-1} \text{ kpc}^{-2}$ for NGC 2276. This is comparable to values found for prototypical starburst outflow galaxies such as NGC 253 and NGC 1482, strongly suggesting that outflows are also taking place in NGC 2276. Furthermore, the kinematics of $\text{H}\alpha$ gas in the disc is consistent with gas motion out of the plane of the galaxy (Gruendl et al. 1993), and the observed steepening of the radio spectral index with frequency is consistent with adiabatic cooling in a galactic wind (Hummel & Beck 1995).

If we assume most of the tail gas originated along the starbursting western edge where it was instantaneously accelerated to the post-shock velocity v_2 , the typical time-scale for this gas to reach the tail region would be ~ 45 Myr. Using the stellar population synthesis models of Bruzual & Charlot (2003), we find that even a $10 M_{\odot} \text{ yr}^{-1}$ starburst of this age can easily be accommodated by the present optical broad-band colours of NGC 2276. The resulting mass loss due to SN-driven outflows is not easily estimated, as it depends not only on the average mass expelled by each SN, but also on the amount of ISM swept up by the expanding hot bubbles (the ‘mass-loading’ of the outflow), and on the fraction of outflowing gas that can eventually escape the disc. However, observational studies of starburst outflows in spiral galaxies suggest that, at star formation rates below a few times $10 M_{\odot} \text{ yr}^{-1}$, the mass outflow rate is comparable to the star formation rate (Martin 1999; Rupke, Veilleux & Sanders 2005). This would suggest an upper limit to the outflow mass loss rate of $\sim 5 M_{\odot} \text{ yr}^{-1}$ for NGC 2276. We therefore conclude that a scenario in which starburst outflows are being swept back by ram pressure provides a possible explanation for some, potentially all, of the hot tail gas.

The X-ray tail thus does seem likely to be ISM displaced from the disc by transport processes. If the hot tail gas did indeed originate in the $T \approx 0.5$ keV starburst-generated gas that probably dominates the disc X-ray emission, one could ask whether any mechanism could heat hot disc gas from this temperature to the tail temperature of $T_{\text{tail}} \approx T_{\text{IGM}} \approx 0.8$ keV within the relevant time-scales. We can first obtain an order-of-magnitude estimate of the time-scales involved for conductive heating from the IGM, assuming heating between the above temperatures over a length-scale of ~ 5 kpc (from the projected edge to the centre of the tail). The scalelength of the temperature gradient $l_T = T/|\nabla T| \sim 10$ kpc, much longer than the electron mean free path $\lambda_e \approx 0.3(T/\text{keV})^2(n_e/10^{-3} \text{ cm}^{-3})^{-1}$ kpc, which is at most a few hundred pc. Heat conduction at the Spicer rate (Sarazin 1988) would then proceed on a time-scale

$$t_{\text{cond}} \sim 0.2 \left(\frac{n_e}{10^{-3} \text{ cm}^{-3}} \right) \left(\frac{l_T}{\text{kpc}} \right)^2 \left(\frac{T}{\text{keV}} \right)^{-5/2} \text{ Myr}, \quad (13)$$

of order $t_{\text{cond}} \sim 100$ Myr. Given the complexity of the problem, this is only a rough estimate, since gas would be heated while being displaced from the disc (changing l_T), turbulence could act to mix IGM and disc gas, and magnetic fields in and above the disc could be suppressing heat conduction by some unknown factor (cf. the presence of cold fronts observed in some clusters of galaxies, see, e.g., Vikhlinin, Markevitch & Murray 2001). While bearing these caveats in mind, we note that the galaxy would have moved 5 kpc in only ~ 10 Myr, suggesting that the tail cannot be

conductively heated gas as the time-scale for this is too long. Further, if the tail were galactic gas heated by conduction, then magnetic fields should be unimportant in the tail region, which appears inconsistent with the presence of significant radio continuum emission (Fig. 5). A more promising heating mechanism is shock heating, which could raise T by a factor ~ 1.7 (cf. equation 2), consistent with hot disc gas being heated from ~ 0.5 to ~ 0.8 keV. But heating may, in fact, not be required at all; a small fraction of tail gas could be the very hot, tenuous component of starburst outflows predicted by hydrodynamical simulations of such outflows (Strickland & Stevens 2000).

A plausible explanation for the X-ray tail is therefore that it represents hot disc gas originating in supernova outflows, mildly shocked and removed from the disc by ram pressure. We note that the tail is unlikely to be shock-heated *cold* disc gas, as the pressure of the cold ISM is larger than the combined thermal and ram pressure of the IGM. A collision between a fragment of the cold, dense ISM and the IGM would form a shock in the latter rather than significantly heating the cold disc gas.

Summarizing, the X-ray tail indicates a mass loss rate of $\dot{M}_{\text{tail}} \sim 3\text{--}6 M_{\odot} \text{ yr}^{-1}$ of hot gas. The two mechanisms of viscous stripping and starburst outflows could each be responsible for the loss of $\sim 5 M_{\odot} \text{ yr}^{-1}$ of gas, and so can each explain the amount of hot gas in the tail. Other processes, such as tidal interactions or Bondi-Hoyle accretion, do not appear to be favoured by the data. The presence of an HI tail coincident with that seen in X-rays suggests that cold gas is also being removed from the disc at a rate of $\sim 2 M_{\odot} \text{ yr}^{-1}$, probably by viscous stripping rather than ram pressure. Our mass model of the galaxy suggests that this cold gas would remain bound in the potential of NGC 2276. This implies that most ($\sim 60\text{--}100$ per cent) of the gas escaping the galaxy is in a hot phase, the exact fraction depending on how much of the HI in the tail remains bound. We note that, owing to the strong dominance of HI gas over X-ray gas in the disc, most of the gas stripped by viscous stripping would be expected to be in a cold phase. The overall picture could therefore be one in which viscous stripping is mainly removing cold disc gas, whereas ram pressure acting on starburst outflows removes the hot starburst-generated gas, with some of the stripped gas being subsequently heated by shocks. From our X-ray data alone we cannot constrain the relative importance of these two processes for the hot gas; the only safe conclusion is that they could have a comparable impact. It seems possible, however, that star formation could have an important indirect effect on the efficiency of viscous stripping, by making the hot disc gas more vulnerable to the effects of hydrodynamical instabilities. Only dedicated simulations could quantify the importance of this effect.

4.4 Importance of tidal interactions

Evidence of gravitational interactions between NGC 2276 and the nearby group elliptical NGC 2300 have been reported, suggesting that IGM interactions may not be solely responsible for the observed features of this spiral (see Gruendl et al. 1993; Davis et al. 1997). The aim of this section is to address the question of whether tidal interactions are really necessary to explain the features of NGC 2276, and if so, whether their importance can be constrained. This per-

tains mainly to the compression of the stellar and gaseous material along the western edge, as we have just shown that the eastern gas tail is unlikely to have a tidal origin.

There are essentially three separate claims of evidence for an ongoing or past tidal interaction between NGC 2276 and NGC 2300: (i) Forbes & Thomson (1992) claim that NGC 2300 has a tidal extension, interpreting this as evidence of a past interaction with NGC 2276; (ii) Gruendl et al. (1993) argue that certain peculiar features of the velocity field of H α emitting disc gas are hard to explain by ram pressure and therefore must have a tidal origin; (iii) the fact that the stellar disc, in particular the older population of stars dominating the R -band light, has a truncated distribution similar to that of the HI and H α emission, suggests that this could not have been induced by the present ram pressure and so again must have a tidal origin. The claims are backed by the more indirect arguments that ram pressure is probably not strong enough to induce the observed peculiarities of NGC 2276, such as the truncation of the stellar and gaseous discs and the enhanced star formation along the W edge. In line with this, the model results of Fujita & Nagashima (1999) suggest that ram-pressure compression of gas cannot lead to an enhancement in the star formation rate by more than a factor of 2, even for galaxies falling through cluster centres. If so, the strong star formation of NGC 2276 may require a tidal origin. Tidal interactions *can* enhance the star formation rate (e.g. Kennicutt et al. 1987), although it remains unclear whether they can cause an order-of-magnitude increase as could be the case for NGC 2276 (Mihos, Richstone & Bothun 1991).

However, there are several lines of evidence which suggest that tidal interactions may not be essential to explaining the properties of NGC 2276. Firstly, assuming NGC 2300 is stationary in the group potential, it is questionable whether tidal interactions are really very efficient at a relative velocity of $v_{\text{gal}} \sim 850 \text{ km s}^{-1}$. Secondly, the tidal extension of NGC 2300 reported by Forbes & Thomson (1992) is claimed to protrude towards the north-east, and is thus not in the direction of the present projected position of NGC 2276. Thirdly, regarding the peculiar velocity field of H α gas in the disc of NGC 2276, as Gruendl et al. (1993) note themselves, the kinematics of this H α gas can also be explained by gas motion out of the plane of the galaxy, and it is not strictly necessary to invoke a tidal origin. Given the very likely presence of starburst outflows, this interpretation seems at least as attractive.

Another issue is the question of whether tidal interactions must be invoked to explain the truncation of the R -band light along the W edge, and whether the strong star formation along this edge can be associated with such interactions. It is clear that ram pressure compression of molecular cloud complexes could lead to enhanced star formation along the W edge. If a factor ~ 2 increase in the star formation rate (SFR) can be obtained this way (Fujita & Nagashima 1999), then the SFR prior to the IGM interaction should have been $\sim 1\text{--}3 M_{\odot} \text{ yr}^{-1}$. This is not an unreasonably high value, and observations of galaxies falling into the cluster A1367 (Gavazzi et al. 1995) suggest that SFR enhancements at even stronger levels can indeed result from ICM interactions. Even more pertinent is the fact that the time since closest approach with NGC 2300 is $\gtrsim 80$ Myr and hence larger than the typical age of massive stars dom-

inating the B -band light. The current high SFR is therefore unlikely to have been triggered exclusively by tidal interactions. As for the truncation of the stellar disc, if young stars are preferentially formed in regions where external pressure contributes to the compression of molecular gas, then B -band and $H\alpha$ light should trace the cold gas morphology, as observed. The red and near-infrared light, arising predominantly from an older stellar population, could be truncated if the IGM interaction has persisted for sufficiently long, perhaps several 10^8 yr. There is a clear indication that also the JHK isophotes are compressed along the W edge (albeit far less strongly than the blue light). The position and derived 3-D velocity of NGC 2276 implies that the galaxy has been within the group virial radius of ~ 1 Mpc (Davis et al. 1996) for at least ~ 1 Gyr and possibly much longer. It therefore seems possible that NGC 2276 has experienced considerable ram pressure for several 10^8 yr, so a tidal origin for the truncation of R -band light is not necessarily favoured over ram pressure compression.

Tidal interactions should also lead to centrally peaked SFR enhancements (e.g., Keel et al. 1985; Barnes & Hernquist 1996; Bergvall, Laurikainen & Aalto 2003), contrary to what is observed for NGC 2276. Even so, gas should recover from tidal distortions on a sound crossing time-scale, which, even for a 5 kpc structure, is only ~ 10 Myr at the temperature of the hot ISM. This is far shorter than the time since closest approach between NGC 2276 and NGC 2300, so only some long-lasting dynamical excitation triggered by the interaction could be maintaining the W structure.

From these arguments, it appears that the tidal scenario on its own faces too many difficulties to be able to explain the morphology of NGC 2276. We cannot rule out that gravitational effects have played a role in shaping the properties of this galaxy, but they seem unlikely to be dominant. On the other hand, a combination of ram-pressure (acting for several tens, perhaps hundreds, of Myr) and starburst outflows provides a natural explanation for the enhanced star formation primarily along the W edge, the compression of radio, $H\alpha$, broad-band optical/near-infrared, and X-ray isophotes along this edge, the origin and properties of the eastern gas tail, and the $H\alpha$ kinematics in the disc.

5 IMPLICATIONS FOR GALAXY EVOLUTION IN GROUPS

There is strong evidence (e.g. Jones, Smail & Couch 2000; Bicker, Fritze-v. Alvensleben & Fricke 2002) that spirals in rich clusters of galaxies are transformed into S0 galaxies by interactions with the cluster environment, a process underlying part of the well-known morphology–density relation seen in clusters (but see also Burstein et al. 2005). The fact that such a relation exists also for groups (Helsdon & Ponman 2003) shows that the underlying mechanisms are also at work in group environments. The relation appears to be stronger in groups with a detectable hot intragroup medium than in those without (Osmond & Ponman 2004), but this may only reflect an increased efficiency of the relevant processes in collapsed systems, not necessarily a connection with the presence of hot, dense gas.

The HI deficiency of NGC 2276 mentioned in Sec-

tion 1 suggests that this galaxy could already have lost an amount of disc gas comparable to the current HI supply of $6.4 \times 10^9 M_\odot$, and that stripping processes *are* acting in this system. If the present mass loss rate of $\dot{M}_{\text{tail}} \approx 3\text{--}6 M_\odot \text{ yr}^{-1}$ is representative, then NGC 2276 could have been losing HI for $\sim 1\text{--}2$ Gyr (comparable to the sound crossing time of the group) and will have exhausted its supply in another $\sim 1\text{--}2$ Gyr. This indicates that galaxies in groups could lose all atomic gas over the course a few Gyr as a result of gas stripping by the intragroup medium. While this is much slower than in rich cluster cores, where such processes are expected from simulation results to take place on time-scales of tens of Myr (Abadi et al. 1999; Quilis et al. 2000), it could still be sufficiently rapid to have made a significant impact on the galaxy population in most groups that have now collapsed. This is particularly true for cluster galaxies, as these were incorporated into groups first and can have experienced such interactions for a significant fraction of a Hubble time. A well-known example, whose origin could be at least partly explained by such stripping processes, is the HI deficient spirals seen in the outskirts of the Virgo cluster (Sanchis et al. 2004).

Star formation, interaction-induced or not, will contribute to exhausting the gas supply of spirals; for NGC 2276, the current star formation rate of $\sim 5 M_\odot \text{ yr}^{-1}$ suggests that interaction-induced star formation may, at least temporarily, be as important as stripping itself in exhausting the gas supply of spirals in dense environments (although some of the gas going into star formation will be returned to the ISM on time-scales of $\sim 10^7$ yr). The question remains whether such starburst activity is needed to facilitate gas loss from group galaxies. This cannot be unambiguously addressed by the present study, as both the observed X-ray and HI tails of NGC 2276 could be accounted for by viscous stripping alone. An indication that starburst outflows are not a *prerequisite* for mass loss in groups is the fact that certain group galaxies, such as Holmberg II (Bureau & Carignan 2002) and NGC 2820 (Kantharia et al. 2005), also appear to be losing gas because of ram pressure or viscous stripping, without showing any signs of starburst activity. A 22 ks *ROSAT* study with a limiting point source sensitivity of $\sim 10^{37} \text{ erg s}^{-1}$ found no diffuse X-ray gas in Holmberg II (Kerp, Walter & Brinks 2002), implying that any X-ray tail of this galaxy is orders of magnitude fainter than the $2 \times 10^{39} \text{ erg s}^{-1}$ found for the NGC 2276 tail. However, based on its B -band luminosity of $1.3 \times 10^9 L_\odot$ (Tully 1988) and the relation of Read & Ponman (2001), Holmberg II is expected to show a total diffuse X-ray luminosity of $\sim 2 \times 10^{37} \text{ erg s}^{-1}$. Any X-ray tail of this galaxy would therefore likely remain undetected in the *ROSAT* data. Furthermore, since we are not aware of any dedicated X-ray studies of the gas tail in NGC 2820, we cannot reliably compare the exact extent to which these two galaxies contain hot tail gas with our corresponding results for NGC 2276.

In the case of a fairly massive spiral like NGC 2276, another important effect of ram pressure is its ability to prevent any coronal gas from cooling out on to the disc. This would eventually quench star formation by cutting off the supply of fresh material for this process. Further, since the stripping radius will decrease with time, because gas is continuously lost from the galaxy via starburst outflows (hence reducing Σ_g in equation 10), NGC 2276 would become in-

creasingly bulge-dominated with time. The indication, mentioned in Section 4.2, that gas in the W disc is currently being swept inward, suggests that the bulge itself could be growing at present. The end product would be a galaxy with virtually no atomic gas, little star formation, a large bulge-to-disc ratio, and potentially a more luminous bulge. These properties are similar to those of S0 galaxies, suggesting that ram pressure could be an important mechanism to form such galaxies. We note that the NGC 2300 group already harbours an S0 galaxy, IC 455 (Mulchaey et al. 1993), so whichever mechanisms are at work in the transformation of galaxies into S0's, they have previously been successful in this environment. Thus, while there is evidence both for (e.g. Vogt et al. 2004) and against (e.g. Goto 2005) ram pressure driving the morphological evolution of cluster spirals into S0's, our results for NGC 2276 indicate that ram pressure could at least be a contributing factor, even in environments where it was earlier thought to be inefficient.

Another class of objects worth mentioning in this context is the so-called 'E+A' galaxies, believed to be post-starburst galaxies which have had their starburst activity abruptly truncated within the past Gyr. The origin of this rapid halt to their star formation is poorly understood, but as these galaxies are known to exist also in groups (Blake et al. 2004), they could have had their recent evolution affected by hot intragroup gas. However, our estimated time-scale for stripping via IGM interactions in groups of several Gyr suggests that this process is too slow to provide an important route to forming such objects. This would be consistent with recent results attributing the origin of E+A galaxies predominantly to galaxy-galaxy interactions and mergers (Yamauchi & Goto 2005).

6 CONCLUSIONS

A 45 ks *Chandra* exposure of the spiral NGC 2276 in the NGC 2300 group of galaxies has revealed a shock-like feature along the western edge of the galaxy and a low-surface-brightness tail extending in the opposite direction. The X-ray morphology of NGC 2276 resembles that seen at optical and radio wavelengths and is suggestive of supersonic motion of the galaxy through the ambient hot intragroup gas in a direction towards the west. X-ray imaging spectroscopy reveals evidence of a build-up of thermal pressure at the leading western edge of the galaxy, and the density and temperature increase of this gas is consistent with the presence of a shock front due to the galaxy moving at Mach 1.7 ($\sim 850 \text{ km s}^{-1}$) through the surrounding medium. Diffuse X-ray emission with $kT \approx 0.5 \text{ keV}$ is detected across the optical disc, and a number of X-ray bright point sources are seen along the W edge, where strong star formation activity is taking place. Contrary to previous claims, we conclude that tidal interactions are not essential to explaining this star formation activity, nor the morphology of the galaxy as seen across a range of wavelengths.

In order to investigate the effects of ram pressure resulting from the motion of NGC 2276 through the intragroup gas, we have modelled the gravitational potential of the galaxy, and shown that the radius outside which gas can be stripped by ram pressure corresponds well to the observed radius of the gaseous and stellar disc. Ram pres-

sure stripping could therefore have dictated the present size of the disc. Whereas ram pressure itself is probably insufficient to remove significant amounts of cold disc gas from the galaxy, turbulent viscous stripping could be removing $\sim 5 M_{\odot} \text{ yr}^{-1}$. Due to the high star formation rate of the galaxy, starburst outflows are very likely taking place as well, although we cannot confirm this directly from the X-ray data as the galaxy is viewed nearly face-on. We estimate that such outflows could be responsible for an additional mass loss of no more than $\sim 5 M_{\odot} \text{ yr}^{-1}$, and that these outflows would also be strongly affected by ram pressure. As the X-ray tail extending to the east of the galaxy would suggest a mass loss rate of $3\text{--}6 M_{\odot} \text{ yr}^{-1}$, this implies that either of these two mechanisms could explain the presence of this tail. A comparison to existing HI data indicates that cold HI gas is also being removed from the disc, but that most of the gas stripped from the galaxy is currently in a hot phase.

At the present mass loss rate, the current HI supply in the disc of NGC 2276 would be exhausted within 1–2 Gyr. From the present HI content, we further estimate that gas stripping could have been active for the previous ~ 2 Gyr. Hence on reasonably short time-scales – a small fraction of a Hubble time – all HI in this fairly massive spiral could be lost. This strongly suggests that the removal of galactic gas through interactions with the surrounding hot medium *can* be effective in group environments, although, in this particular case, the process is expected to be slower than in cluster cores by two orders of magnitudes. A secondary effect of the ram pressure experienced by NGC 2276 is that it will inhibit the cooling out of any hot coronal gas on to the disc, thus preventing the infall of fresh material for continuous star formation. Combined with the gas loss, this implies that NGC 2276 would eventually evolve into an object with properties not too dissimilar from present-day S0 galaxies. Our results therefore suggest that ram pressure could at least be a contributing factor in the morphological evolution of spirals into S0's, even in environments where this mechanism was earlier thought to be inefficient.

ACKNOWLEDGMENTS

We thank the referee for constructive and insightful comments. This work has made use of the NASA/IPAC Extragalactic Database (NED) and the HyperLeda database. JR acknowledges the support of the European Community through a Marie Curie Intra-European Fellowship under contract no. MEIF-CT-2005-011171. JSM acknowledges partial support from Chandra grant G04-5144X and NASA grant NNG04GC846.

REFERENCES

- Abadi M.G., Moore B., Bower R.G., 1999, MNRAS, 308, 947
- Acreman D.M., Stevens I.R., Ponman T.J., Sakelliou I., 2003, MNRAS, 341, 1333
- Anders E., Grevesse N., 1989, Geochim. Cosmochim. Acta, 53, 197
- Barnes J.E., Hernquist L., 1996, ApJ, 471, 115

- Bergvall N., Laurikainen E., Aalto S., 2003, *A&A*, 405, 31
- Bicker J., Fritze-v. Alvensleben U., Fricke K.J., 2002, *A&A*, 387, 412
- Birnboim Y., Dekel A., 2003, *MNRAS*, 345, 349
- Blake C. et al., 2004, *MNRAS*, 355, 713
- Bruzual G., Charlot S., 2003, *MNRAS*, 344, 1000
- Buote D.A., 2000, *MNRAS*, 311, 176
- Bureau M., Carignan C., 2002, *AJ*, 123, 1316
- Burstein D., Ho L.C., Huchra J.P., Macri L.M., 2005, *ApJ*, 621, 246
- Cayatte V., van Gorkom J.H., Balkowski C., Kotanyi C., 1990, *AJ*, 100, 604
- Davis D.S., Mushotzky R.F., 2004, *ApJ*, 604, 653
- Davis D.S., Mulchaey J.S., Mushotzky R.F., Burstein D., 1996, *ApJ*, 460, 601
- Davis D.S., Keel W.C., Mulchaey J.S., Henning P.A., 1997, *AJ*, 114, 613
- Dickey J.M., Lockman F.J., 1990, *ARA&A*, 28, 215
- Forbes D.A., Thomson R.C., 1992, *MNRAS*, 254, 723
- Fujita Y., Nagashima M., 1999, *ApJ*, 516, 619
- Gavazzi G., Contursi A., Carrasco L., Boselli A., Kennicutt R., Scodreggio M., Jaffe W., 1995, *A&A*, 304, 325
- Gilfanov M., 2004, *MNRAS*, 349, 146
- Giudice G., 1999, in Giuricin G., Mezzetti M., Salucci P., eds, *ASP Conf. Ser. 176: Observational Cosmology: The Development of Galaxy Systems Vol. 176*, Bolzano, p. 136
- Gonzalez A.H., Tran K.-V.H., Conbere M.N., Zaritsky D., 2005, *ApJL*, 624, L73
- Goto T., 2005, *MNRAS*, 359, 1415
- Goto T., Yamauchi C., Fujita Y., Okamura S., Sekiguchi M., Smail I., Bernardi M., Gomez P.L., 2003, *MNRAS*, 346, 601
- Grevesse N., Sauval A.J., 1998, *Space Sci. Rev.*, 85, 161
- Gruendl R.A., Vogel S.N., Davis D.S., Mulchaey J.S., 1993, *ApJL*, 413, L81
- Gunn J.E., Gott J.R. III, 1972, *ApJ*, 176, 1
- Haynes M.P., Giovanelli R., 1984, *AJ*, 89, 758
- Helsdon S.F., Ponman T.J., 2003, *MNRAS*, 339, L29
- Henry J.P., Finoguenov A., Briel U.G., 2004, *ApJ*, 615, 181
- Homeier N.L. et al., 2006, *AJ*, 131, 143
- Hummel E., Beck R., 1995, *A&A*, 303, 691
- Irwin J.A., Athey A.E., Bregman J.N., 2003, *ApJ*, 587, 356
- Jones L., Smail I., Couch W., 2000, *ApJ*, 528, 118
- Kantharia N.G., Ananthakrishnan S., Nityananda R., Hota A., *A&A*, 435, 483
- Keel W.C., Kennicutt R.C., Hummel E., van der Hulst J.M., 1985, *AJ*, 90, 708
- Kennicutt R.C., Jr., 1998, *ApJ*, 498, 541
- Kennicutt R.C., Jr., Roettiger K.A., Keel W.C., van der Hulst J.M., Hummel E., 1987, *AJ*, 93, 1011
- Kerp J., Walter F., Brinks E., 2002, *ApJ*, 571, 809
- Landau L.D., Lifshitz E.M., 1987, *Fluid mechanics*, 2nd edition, Pergamon Press, Oxford
- Lewis I., et al., 2002, *MNRAS*, 334, 673
- Machacek M., Dosaj A., Forman W., Jones C., Markevitch M., Vikhlinin A., Warmflash A., Kraft R., 2005a, *ApJ*, 621, 663
- Machacek M., Nulsen P., Stirbat L., Jones C., Forman W., 2005, *ApJ*, 2005b, *ApJ*, 630, 280
- Mannucci F., Della Valle M., Panagia N., Cappellaro E., Cresci G., Maiolino R., Petrosian A., Turatto M., 2005, *A&A*, 433, 807
- Martin C.L., 1999, *ApJ*, 513, 156
- Mihos J.C., Richstone D.O., Bothun G.D., 1991, *ApJ*, 377, 72
- Mulchaey J.S., Davis D.S., Mushotzky R.F., Burstein D., 1993, *ApJL*, 404, L9
- Nulsen P. E. J., 1982, *MNRAS*, 198, 1007
- Osmond J.P.F., Ponman T.J., 2004, *MNRAS*, 350, 1511
- Quilis V., Moore B., Bower R., 2000, *Science*, 288, 1617
- Rasmussen J., Sommer-Larsen J., Pedersen K., Toft S., Benson A., Bower R.G., Olsen L.F., 2006, *ApJ*, submitted
- Read A.M., Ponman T.J., 2001, *MNRAS*, 328, 127
- Rosenberg J.L., Schneider S.E., 2002, *ApJ*, 567, 247
- Roediger E., Hensler G., 2005, *A&A*, 433, 875
- Rupke D.S., Veilleux S., Sanders D.B., 2005, *ApJS*, 160, 115
- Sakelliou I., 2000, *MNRAS*, 318, 1164
- Sanchis T., Mamon G.A., Salvador-Solé E., Solanes J.M., 2004, *A&A*, 418, 393
- Sarazin C.L., 1988, *X-ray Emission from Clusters of Galaxies*, Cambridge Univ. Press, Cambridge
- Sivakoff G.R., Sarazin C.L., Carlin J.L., 2004, *ApJ*, 617, 262
- Stevens I.R., Acreman D.M., Ponman T.J., 1999, *MNRAS*, 310, 663
- Strickland D.K., Stevens I.R., 2000, *MNRAS*, 314, 511
- Strickland D.K., Heckman T.M., Colbert E.J.M., Hoopes C.G., Weaver K.A., 2004, *ApJ*, 606, 829
- Sun M., Vikhlinin A., 2005, *ApJ*, 621, 718
- Toft S., Rasmussen J., Sommer-Larsen J., Pedersen K., 2002, *MNRAS*, 335, 799
- Tully R.B., 1988, *Nearby Galaxies Catalog*, 1988, Cambridge Univ. Press, Cambridge
- van der Meer A., Kaper L., di Salvo T., Mendez M., van der Klis M., Barr P., Trams N.R., 2005, *A&A*, 432, 999
- Verdes-Montenegro L., Yun M.S., Williams B.A., Huchtmeier W.K., Del Olmo A., Perea J., 2001, *A&A*, 377, 812
- Vikhlinin A., Markevitch M., Murray S.S., 2001, *ApJL*, 549, L47
- Vogt N.P., Haynes M.P., Giovanelli R., Herter T., 2004, *AJ*, 127, 3300
- Vollmer B., Beck R., Kenney J.D.P., van Gorkom J.H., 2004, *AJ*, 127, 3375
- Young J.S., Xie S., Kenney J.D.P., Rice W.L., 1989, *ApJS*, 70, 699
- Wang Q.D., Owen F., Ledlow M., 2004, *ApJ*, 611, 821
- White S.D.M., Frenk C.S., 1991, *ApJ*, 379, 52
- Yamauchi C., Goto T., 2005, *MNRAS*, 359, 1557

This paper has been typeset from a \TeX / \LaTeX file prepared by the author.